Astron. Astrophys. 352, L99–L102 (1999)

ASTRONOMY AND ASTROPHYSICS

LETTER

Letter to the Editor

New insight into transition region dynamics via SUMER observations and numerical modelling

L. Teriaca[1], **J.G. Doyle**[1], **R. Erdélyi**[2], **and L.M. Sarro**[3]

[1] Armagh Observatory, College Hill, Armagh BT61 9DG, Northern Ireland (lte,jgd@star.arm.ac.uk)
[2] Space and Atmosphere Research Center, Department of Applied Mathematics, University of Sheffield, England (Robertus@sheffield.ac.uk)
[3] Laboratorio de Astrofisica Espacial y Fisica Fundamental (LAEFF) INTA, 28080 Madrid, Spain

Received 11 October 1999 / Accepted 2 November 1999

Abstract. We explore the idea that the occurrence of nano-flares in a magnetic loop around the O VI formation temperature could explain the observed red-shift of mid-low transition region lines as well as the blue-shift observed in low coronal lines ($T > 6 \times 10^5$ K). Observations are compared to numerical simulations of the response of the solar atmosphere to an energy perturbation of 4×10^{24} ergs representing an energy release during magnetic reconnection in a 1-D semi-circular flux tube. The temporal evolution of the thermodynamic state of the loop is converted into C IV 1548, O VI 1032 and Ne VIII 770 line profiles in non-equilibrium ionization. Performing an integration over the entire period of simulations, a redshift of ~ 6 km s^{-1} is found in C IV, while a blue-shift of $\sim 2\,\mathrm{km\,s^{-1}}$ and $\sim 10\,\mathrm{km\,s^{-1}}$ were derived for O VI and Ne VIII, respectively, in reasonable agreement with observations.

Key words: Magnetohydrodynamics (MHD) – line: profiles – Sun: activity – Sun: corona – Sun: transition region – Sun: UV radiation

1. Introduction

During the last two decades, observations of red-shifted emission lines formed at transition region (TR) temperatures were obtained by many authors using several UV instruments with different spatial resolution (see Brekke et al. 1997 and references therein). Brekke et al. (1997) and Chae et al. (1998a) have shown that for the 'quiet' Sun the red-shift is peaked around 1.5×10^5 K with a value of 11 km s^{-1} . Their data suggested it to be also present at higher temperatures with a value of around 5 km s^{-1} for Ne VIII 770 Å in the 'quiet' Sun. On-the-other-hand, Peter & Judge (1999) found *blue-shifts* at disk center for three coronal lines (i.e., Ne VIII at 770 Å and 780 Å and Mg X at 625 Å). This difference in the value of Doppler shift for Ne VIII 770 is due to the assumption of a new rest wavelength of 770.428 Å, confirmed by Dammasch et al. (1999). Recently, Teriaca et al. (1999) found evidence for *blue-shift* in both the 'quiet' Sun and in an active region at upper TR and coronal temperatures.

In this Letter we investigate the consequences of these observational results via a comparison with numerical studies. The simulations were carried out representing a reconnection-type of physical process with the calculations being converted into UV line profiles in non-equilibrium ionization (see Erdélyi et al. 1998, 1999, Sarro et al. 1999 for earlier work in relation to the modelling of UV explosive events).

2. Observational results

Teriaca et al. (1999) have shown that the temperature variations of the Doppler shifts and non-thermal velocities in the 'quiet' Sun and active region have important implications for the validity of the physical models for the red-shift (or down-flow) problem. In Fig. 1 we show the behaviour of the Doppler shift versus temperature of formation both for a 'quiet' Sun and an active region as reported by Teriaca et al. (1999). From their measurements it is possible to infer that the Doppler shift reversal from red-shift to blue-shift takes place around $log\,T = 5.7$ (5×10^5 K) in the active region while in the 'quiet' Sun a value between $log\,T = 5.7$ and $log\,T = 5.75$ (5.0×10^5 - 5.6×10^5 K) can be estimated.

3. Modelling

There are a few different models in the literature which attempt to explain the down-flow problem, e.g., the return of spicular material, siphon flows through loops, nano-flares and explosive events (see Brekke et al. 1997; Peter & Judge 1999, Sarro et al. 1999 and reference therein). Out of all these we found the most relevant and consistent with our observations is the one by Hansteen (1993). He considers nano-flares occurring at the top of coronal loops, generating MHD waves that propagate downward along the magnetic fields towards and through the transition region.

This model was extended by Hansteen et al. (1996) including the reflection that the chromosphere exerts on the down-

Send offprint requests to: L. Teriaca

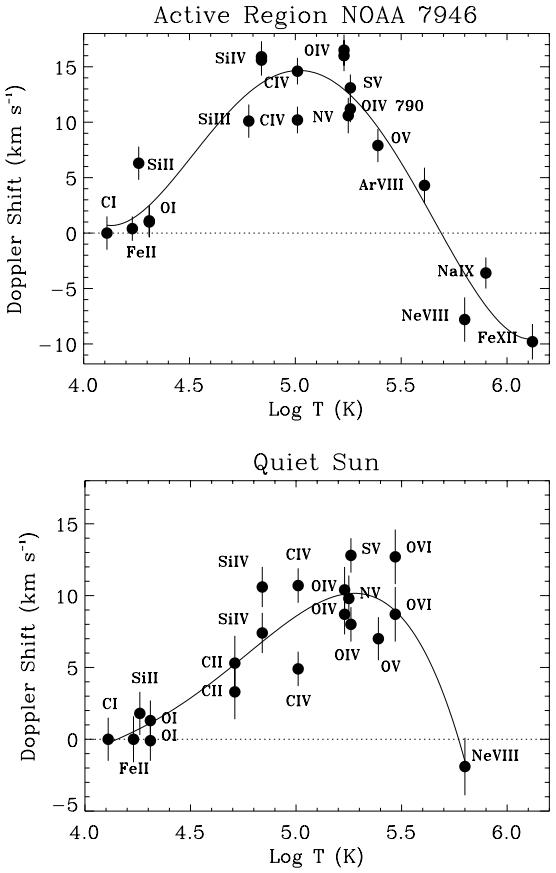

Fig. 1. SUMER measurement of radial velocities in active region NOAA 7946 (top panel) and in the 'quiet' Sun (lower panel). The solid line represent a polynomial fit (Teriaca et al. 1999).

ward travelling waves. Also this model predicts red-shifts in the 'quiet' Sun of ~ 15 km s^{-1} at the C III formation temperature (8×10^4 K) and blue-shifts of ~ -15 km s^{-1} at the Mg IX formation temperature (10^6 K). These are large with respect to the 'quiet' Sun results (see Fig. 1). However, it is able (as also pointed out by Peter & Judge 1999) to explain the presence of blue-shift together with red-shift within one model.

Following the suggestion of Peter & Judge (1999) we support the idea of the prevalent occurrence of magnetic reconnection around the O VI formation temperature (3×10^5 K) as a source for the red-shift observed in the low and middle transition region and for the blue-shift seen in the upper transition region and coronal lines. This can also explain the peak of the non-thermal velocity versus temperature curves at the O VI formation temperature (see Chae et al. 1998b; Teriaca et al. 1999). From this point of view the larger range of values detected for the active region could be explained in terms of a higher frequency of occurrence and/or energy of nano-flares events in the active region with respect to the 'quiet' Sun.

4. Hydrodynamical simulations

The Doppler shifts are interpreted as the response of the solar atmosphere to a sudden release of energy (e.g., reconnection). However, the ultimate origin of the input energy that drives these flows of material has not yet been established (e.g., we do not exclude an explanation based on wave theory especially nonlinear MHD waves).

In the present work the small-scale energy depositions are simulated in a one-dimensional semi-circular rigid magnetic flux tube (see, e.g., Sterling et al. 1991,1993, Mariska 1992, Sarro et al. 1999). The distance along the loop is s, with $s = 0$ fixed at the left boundary of the tube. The length of the loop is taken to be 13,000 km, with a chromosphere 1,500 km thick at both ends of the loop. Gravity forces, $g(s) = g_0 \cos\alpha$, are taken into account, where $g_0 = g\mid_{s=0} = 2.7 \times 10^2$ m s^{-2} and α denotes the angle between the component of gravity along the loop at point s, and the gravity vector downwards. The governing equations of physical processes in the loop can be written in the form:

$$\frac{\partial \rho}{\partial t} + \frac{\partial(\rho v)}{\partial s} = 0, \tag{1}$$

$$\frac{\partial(\rho v)}{\partial t} + \frac{\partial(\rho v^2)}{\partial s} = -\rho g(s) - \frac{\partial p}{\partial s}, \tag{2}$$

$$\frac{\partial E}{\partial t} + \frac{\partial}{\partial s}\left[(E+p)v - \kappa\frac{\partial T}{\partial s}\right] = -\rho v g(s) - L + S, \tag{3}$$

where

$$E = \frac{1}{2}\cdot\rho v^2 + \frac{p}{\gamma - 1}. \tag{4}$$

Here L denotes the radiative loss function and S denotes the volume heating rate. For the radiative loss function we use the analytical expression given by Sterling et al. (1991), while for the input heating rate we take a constant value per unit volume of 3.6×10^{-4} ergs cm^{-3} s^{-1}.

Eqs. (1)–(3) are solved using the Fortran 90 code **EMMA_D** (De Sterck et al. 1998) based on high resolution shock capturing schemes and an approximate Riemann solver. We use a fixed grid spacing corresponding to 13 km per grid cell. The code is implemented with solid wall boundary conditions. At both footpoints, the temperature and the pressure are fixed at 10,000 K and 2.1 dyn cm^{-2}, respectively. After the hydrodynamics variables are computed, we calculate the ion populations for three different ions, and finally a line synthesis program gives UV line profiles suitable for comparison with observations (see §5).

5. Observational consequences

In order to calculate the ion populations along the loop for a given time we have to integrate the ionization equations, i.e.,

$$\frac{\partial N_i}{\partial t} + \frac{\partial(N_i \cdot v)}{\partial s} = N_e(N_{i+1}\alpha_{i+1} + N_{i-1}S_{i-1} - N_i(\alpha_i + S_i)) \tag{5}$$

where α_i and S_i are the recombination and ionization coefficients of ionization stage i and N_i is the volume number density of ion i. From the observed Doppler shifts in Fig. 1 we have

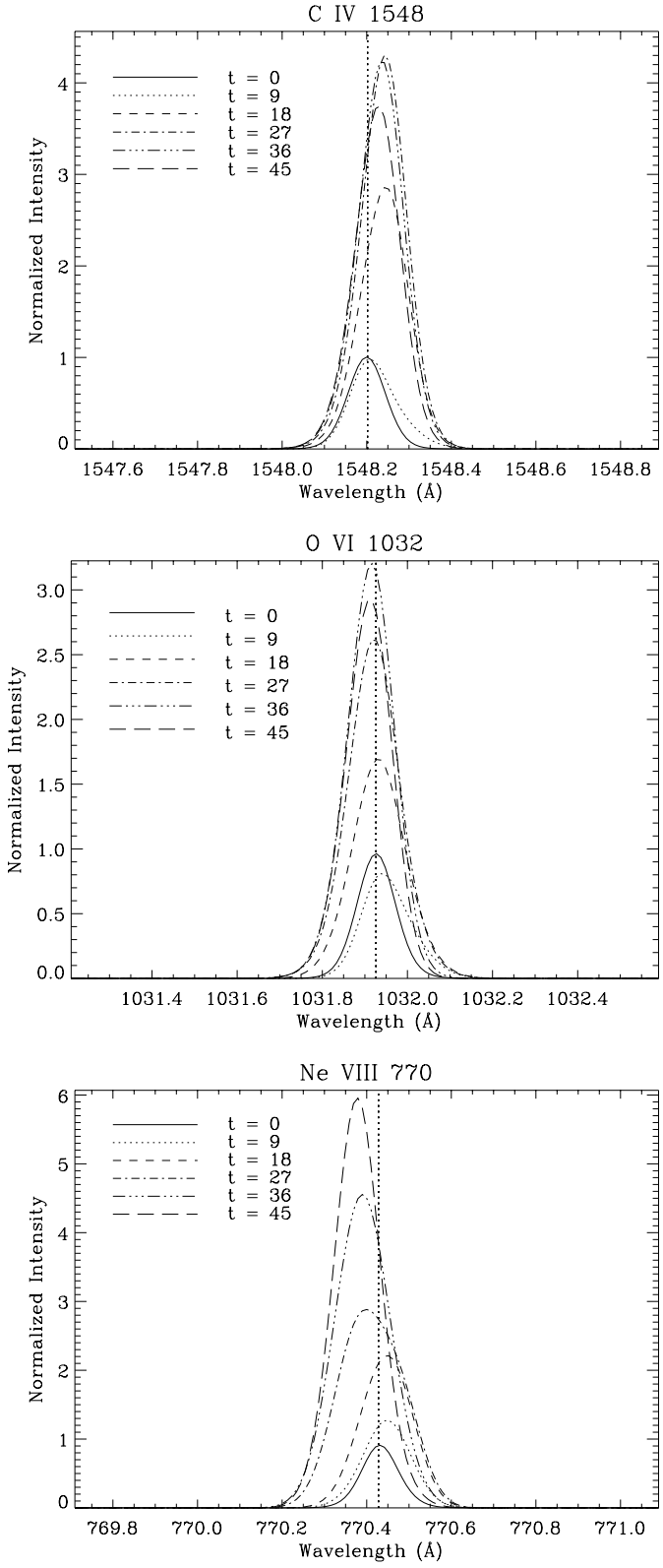

Fig. 2. Response to an energy perturbation representing the energy release during a nano-flare, in a 1-D semi-circular magnetic loop. The temporal evolution of the thermodynamic state of the loop is converted into C IV 1548 Å (top panel), O VI 1032 Å (mid panel) and Ne VIII 770 Å (bottom panel) line profiles (integrated over 9 consecutive seconds) in non-equilibrium ionization.

selected the resonance line of C IV at 1548 Å, O VI 1032 Å, and Ne VIII 770 Å whose ion populations is going to be determined. This offers an easy comparison of Doppler shift observations and numerical predictions of the time evolution of observational signatures. Analyses also show that it is evident that strong deviations from the equilibrium values of the ion populations occur. We do not represent here a careful study of this deviation. We refer the detailed analysis of the evolution of the fractional ion populations with respect to the equilibrium values to a recent PhD thesis (Sarro 1998) devoted to the study of the evolution of the ionization state of several species in a loop subject to these kinds of energy perturbations.

Once the ion populations are computed, the emissivity of a given emission line per unit interval of wavelength in an optically thin, collisionally excited resonance line can be obtained by using the standard equation

$$E_\lambda \propto \frac{hc}{\lambda}\frac{\Omega}{\omega}\frac{N_1}{N_{\rm ion}}\frac{N_{\rm ion}}{N_{\rm elem}}\frac{N_{\rm elem}}{N_{\rm H}}N_{\rm H}N_{\rm e}\frac{\exp\frac{-W}{K_{\rm b}T}}{\sqrt{T}}\phi(\lambda) \qquad (6)$$

Given a distribution of emissivities along the loop, the total intensity can be calculated as

$$I_\lambda = \int_0^{s_e} E_\lambda ds \qquad (7)$$

where s_e is the total length of the loop.

6. Numerical results

We compare our observations with the response to an energy deposition representing nano-flaring due to reconnection in the high part of a 1-D semi-circular magnetic flux tube (Erdélyi et al. 1998,1999, Sarro et al. 1999). After the hydrodynamical simulations, the calculations are turned into UV line profiles applying the non-equilibrium ionization condition in order to make a direct comparison with observable quantities. Note, the condition of non-equilibrium ionization has a major effect on the line formation as was discussed by Sarro et al. (1999).

In the results shown in Figs. 2 & 3, an energy input of 4×10^{24} ergs was released at an height of 5400 km (corresponding to $\log T = 5.7$) in a 1-D magnetic loop. The temporal evolution of the thermodynamic state of the loop is converted into C IV 1548 Å, O VI 1032 Å and Ne VIII 770 Å line profiles (see Fig. 2).

Further, Fig. 3 shows the time evolution of the total intensity (upper panel) and the central wavelength position (lower panel) for the three modelled UV lines. An analysis of Fig. 3 shows that indeed purely red-shift is produced in C IV while blue-shift is produced during the second part of the simulation in O VI and in Ne VIII. Due to the much higher intensity of the latter two lines during the blue-shift part, this results in a predominance of blue-shift in Ne VIII and to a lesser extent in O VI, which is in agreement with observations. Performing an integration over the entire period of simulations (55 seconds), a redshift of $\sim 6\,{\rm km\,s^{-1}}$ is found in C IV, while a blue-shift of $\sim -2\,{\rm km\,s^{-1}}$ and $\sim -10\,{\rm km\,s^{-1}}$ were derived for O VI and Ne VIII, respectively. This is in reasonable agreement with recent observations.

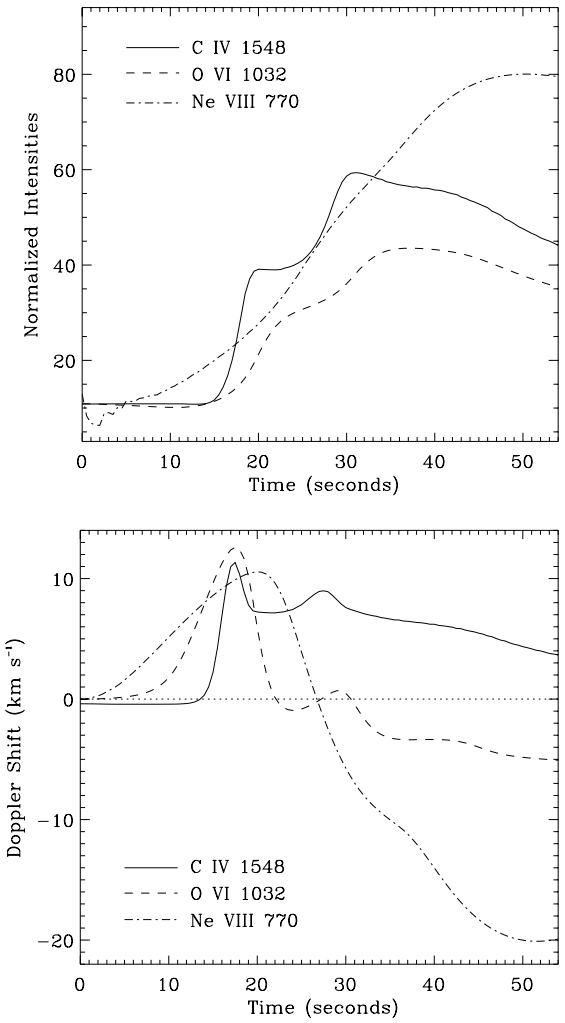

Fig. 3. Time evolution of the total intensity (upper panel) and of the central position (lower panel) for the three modelled lines.

We trust our results shed further light into the physics and modelling of the complexity of the solar (and stellar) transition region. Furthermore our observations provide clues for the possible role of nano-flare events in the transition region as a suitable source for the observed Doppler shift. We plan to develop the modelling of the nano-flare mechanism exploring in detail the parameter space, calculating the response of the model to different amount of deposited energy at different temperatures. Furthermore, we plan to perform full 2-D MHD simulations, including 2D non-equilibrium ionization in order to determine the role of the magnetic field.

Acknowledgements. Research at Armagh Observatory is grant-aided by the Department of Education for N. Ireland while partial support for software and hardware is provided by the STARLINK Project which is funded by the UK PPARC. This work was partly supported by PPARC grant GR/K43315 and a grant from the British Council - Acciones Integradas (Spain) ref. no. 1814. SUMER is part of SOHO, the Solar and Heliospheric Observatory of ESA and NASA. We would like to thank the referee Nils Brynildsen for his comments. R. Erdélyi thanks M. Kéray for patient encouragement.

References

Brekke P., Hassler D.M. & Wilhelm K., 1997, Sol Phys 175, 349
Chae J., Yun H.S. & Poland A.I., 1998a, ApJ S 114, 151
Chae J. Schühle U. & Lemaire F., 1998b, ApJ 505, 975
Dammasch I.E., Wilhelm K., Curdt W. & Hassler D.M., 1999, A&A 364, 285
De Sterck H., Poedts S. & Goedbloed J.P., 1998, J. of Plasma Phys. 59, 277
Erdélyi R., Sarro L.M. & Doyle J.G., 1998, 'Explosive Events Modelled in the View of SOHO Observations', *ESA SP*, 421, 207
Erdélyi R., Sarro L.M. & Doyle J.G., 1999, 'Observations and Modelling of Small-Scale Energetic Transients in the Solar Atmosphere', *ESA SP*, 446, in press
Hansteen V.H., 1993, ApJ 402, 741
Hansteen V.H., Maltby P., Malagoli A., 1996, in R. D. Bentley, J. T. Mariska (eds.), Magnetic Reconnection in the Solar Atmosphere, ASP Conference Series 111, 116
Mariska J.T., 1992, The Solar Transition Region, Cambridge University Press, Cambridge
Peter H. & Judge P.G., 1999, ApJ 522, 1148
Sarro, L.M., 1998, PhD Thesis
Sarro L.M., Erdélyi R., Doyle J.G. & Pérez M.E., 1999, A&A (in press)
Sterling A.C., Mariska J.T., Shibata K. & Suematu Y., 1991, ApJ 381, 313
Sterling A.C., Shibata K. & Mariska J.T., 1993, ApJ 407, 778
Teriaca L., Banerjee D. & Doyle J.G., 1999, A&A 349, 636